

Formation of Surface Ternary Alloys by Coadsorption of Alkali Metals on Al(111)

S. V. Christensen, J. Nerlov,* K. Nielsen, J. Burchhardt, M. M. Nielsen, and D. L. Adams

Institute of Physics and Astronomy, Aarhus University, DK-8000 Aarhus C, Denmark

(Received 3 October 1995)

Coadsorption of one-quarter monolayer Na with one-quarter monolayer K, Rb, or Cs on Al(111) at 300 K is shown to result in the formation of *surface ternary alloys* with (2×2) unit cells. Chemical shifts in core electron binding energies and quantitative analyses by low energy electron diffraction indicate that the first four surface layers consist in each case of an X-Al-Na sandwich ($X \equiv$ K, Rb, or Cs) on a reconstructed Al substrate layer. The lower layer of the sandwich always contains Na, irrespective of the adsorption sequence.

PACS numbers: 68.35.Bs

Recent experimental [1–16] and theoretical studies [17–22] of the adsorption of alkali metals on Al surfaces have revealed an unexpected richness of structural phenomena for this electronically simple system. The adsorption of Na, K, Rb, and Cs on Al(111) and the adsorption of Na on Al(100) has been shown to lead to a reconstruction of the substrate. In the $(\sqrt{3} \times \sqrt{3})R30^\circ$ (hereafter “ $\sqrt{3}$ ”) structures formed on Al(111), and in the Al(100)- $c(2 \times 2)$ -Na structure, the adsorbed alkali atoms occupy substitutional sites formed by displacement of Al atoms from the first layer of the substrate. For Al(111) the adsorption of a further $1/6$ monolayer (ML) Na on the $\sqrt{3}$ -Na phase leads to the formation of a (2×2) -Na phase, which has been shown [12,20] to be a complicated surface binary alloy, consisting of a Na-Al-Na sandwich on a reconstructed Al substrate.

The present work reports the discovery of still more complicated (2×2) phases formed by coadsorption of $1/4$ ML Na with $1/4$ ML K, Rb, or Cs on Al(111). The structure of each of these phases is shown to consist of an X-Al-Na sandwich on a reconstructed Al substrate, where X stands for K, Rb, or Cs. These phases can be regarded as formed by substitution of the uppermost layer of Na atoms in the Al(111)- (2×2) -Na structure by K, Rb, or Cs, and can therefore be described as *surface ternary alloys*. Surprisingly, the resulting structures are independent of the adsorption sequence. The lower layer of the sandwich always consists of Na, irrespective of whether Na or X is adsorbed first.

The Al(111)- (2×2) -Na/X phases were prepared by sequential evaporation from SAES getter sources with the crystal at room temperature. Core level spectra were measured at room temperature using a Vacuum Generators Clam2 electron spectrometer in a vacuum system attached to a Zeiss SX700 monochromator on beam line 5 at the storage ring ASTRID [23] at Århus. Measurements of the Al- $2p$, Na- $2p$, and Cs- $4d$ core levels were made at a photon energy of 125 eV and measurements of the K- $3p$ and Rb- $4p$ core levels were made at a photon energy of 40 eV. Under these conditions the combined instrumental resolution of the SX700 monochromator and the electron spectrometer was 90 and 70 meV, respectively. LEED

intensity-energy spectra were measured in a separate vacuum chamber with a video-LEED system [11].

A model of the structure of the (2×2) -Na/K phase that results from our analysis of core level and LEED measurements is shown in Fig. 1. The evidence for this structure is described below.

The present analysis of shifts in core level binding energies for the (2×2) -Na/X phases follows the corresponding analysis by Andersen and co-workers [3,8] for the (2×2) -Na phase. In the work cited, the observed shifts in binding energies were interpreted in terms of estimates of the shifts expected for different Al/Na coordinations, and the shifts observed in ancillary experiments involving incorporation of Al atoms in thick films of Na, and involving deposition of Cs on the (2×2) -Na phase at low temperature. The validity of the conclusions drawn for the structure of the (2×2) -Na phase were later substantiated by detailed LEED and theoretical analyses [12].

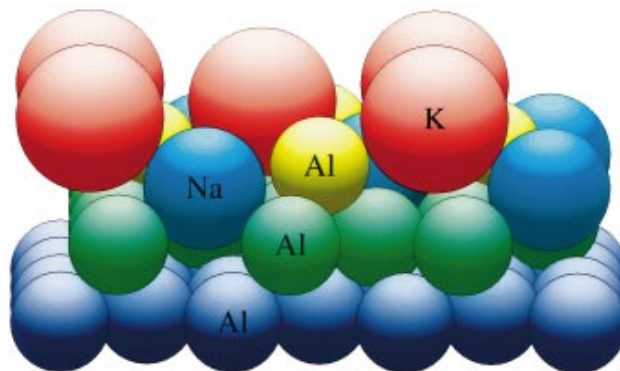


FIG. 1 (color). Side view (tilted 10°) of a model of the Al(111)- (2×2) -Na/K structure. The top four layers, each of (2×2) periodicity, consist of a K-Al-Na sandwich on a reconstructed Al layer with a (2×2) vacancy structure. Na atoms (shown in blue) in the lower layer of the sandwich are located in substitutional sites in the reconstructed layer. Al atoms (shown in yellow) in the sandwich layer and K atoms (shown in red) in the upper layer of the sandwich are located in hcp and fcc sites, respectively, on the reconstructed layer. (Note, however, that the K atoms do not contact Al atoms in the reconstructed layer in the hard-sphere model.) Al atoms in the reconstructed layer are shown in green. Substrate Al atoms are shown in dark blue.

A Na-2*p* spectrum of the (2×2) -Na structure is shown in Fig. 2(a). Two distinct peaks are found at binding energies of $E_b = 30.42$ and 30.93 eV, each consisting of an unresolved spin-orbit doublet, in good agreement with the results of Andersen *et al.* [3,8]. Following the arguments of these authors, these peaks are attributed to the inner and outer layers of sodium, respectively, in a Na-Al-Na sandwich [3,8,12]. The large difference in energy between the two peaks is attributed to the combination of a surface shift and the reduced Na/Al coordination of Na atoms in the outer Na layer as compared to Na atoms in the inner layer. Figure 2(a) also shows a Na-2*p* spectrum for the $\sqrt{3}$ -Na phase. The spectrum contains a single peak at $E_b = 30.78$ eV, close to the binding energy of the outer sodium layer in the (2×2) structure.

Adsorption of 1/4 ML of sodium leads to the formation of a sharp $\sqrt{3}$ LEED pattern, due to the formation $\sqrt{3}$ -Na islands. The Na-2*p* binding energy measured for this phase is the same as for the $\sqrt{3}$ -Na structure at 1/3 ML coverage. Subsequent deposition of potassium at coverages below 1/4 ML results in a LEED pattern which indicates a coexistence of $\sqrt{3}$ and (2×2) phases. The Na-2*p* spectrum of this mixed phase [Fig. 2(b)]

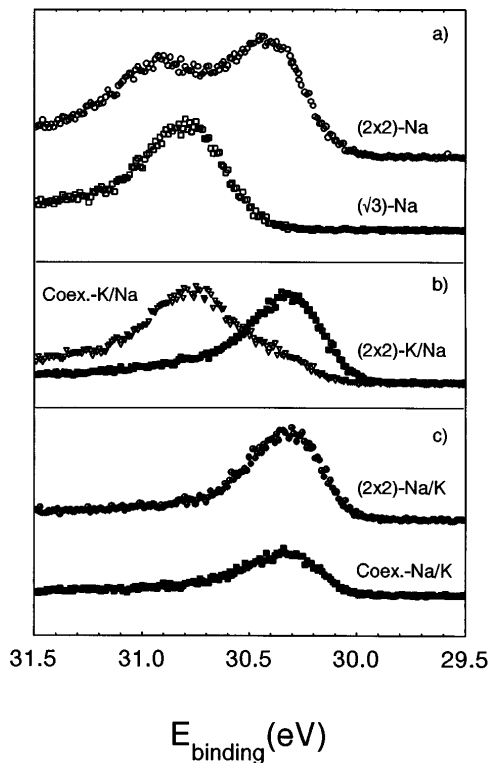


FIG. 2. Na-2*p* core level spectra: (a) for the (2×2) -Na and $(\sqrt{3} \times \sqrt{3})R30^\circ$ -Na phases; (b) for the mixed (2×2) -Na/K phase formed by adsorption of first 1/4 ML Na followed by 1/4 ML K, and for a phase containing coexisting $(\sqrt{3} \times \sqrt{3})R30^\circ$ and (2×2) domains formed by adsorption of 1/4 ML Na followed by 1/10 ML K; (c) for the (2×2) -Na/K phase formed by adsorption of first 1/4 ML K followed by 1/4 ML Na, and for a phase containing coexisting $(\sqrt{3} \times \sqrt{3})R30^\circ$ and (2×2) domains formed by adsorption of 1/4 ML K followed by 1/8 ML Na.

reveals the development of a shoulder at lower binding energy as compared to the corresponding spectrum for the pure $\sqrt{3}$ -Na phase [Fig. 2(a)]. Further deposition to a total potassium coverage of 1/4 ML results in a perfect (2×2) structure. The Na-2*p* spectrum of this (2×2) -Na/K phase [Fig. 2(b)] contains a single peak at a binding energy of $E_b = 30.36$ eV, close to the binding energy of the inner sodium layer in the (2×2) sodium structure. From these observations it can be concluded that the (2×2) -Na/K phase contains an inner layer of sodium and a *separate* outer layer of potassium.

Further structural information can be deduced from corresponding measurements of the Al-2*p* core level, as shown in Fig. 3 for both the (2×2) -Na and (2×2) -Na/K phases. The Al-2*p* spectrum for the (2×2) -Na phase contains two shifted components (indicated by arrows in the figure) at -150 meV (shoulder) and -440 meV with respect to the Al-2*p*_{3/2} peak, which can be attributed [3,8], respectively, to aluminum atoms in the reconstructed outermost layer of the substrate and Al atoms sandwiched between the inner and outer layers of Na. From the strong similarity between the Al-2*p* spectra for the (2×2) -Na and (2×2) -Na/K phases shown in Fig. 3 it can be concluded that the aluminum atoms in the latter structure occupy the same sites as in the pure (2×2) -Na structure. Thus the structure of the (2×2) -Na/K phase, as shown in Fig. 1, is qualitatively the same as the (2×2) -Na phase, except that the outer layer of Na is substituted by K.

In further experiments it was found that reversing the adsorption sequence, i.e., adsorbing 1/4 ML K followed by 1/4 ML Na, also leads to the formation of a (2×2) -Na/K phase, for which Na-2*p* and Al-2*p* spectra are identical to those shown in Figs. 2 and 3. As shown in Fig. 1(c), deposition of Na after adsorption of 1/4 ML K leads to the growth of a Na-2*p* peak at a binding energy corresponding to the formation of an *inner* layer of Na. We conclude, therefore, that Na atoms burrow under the K layer to produce the same structure (Fig. 1)

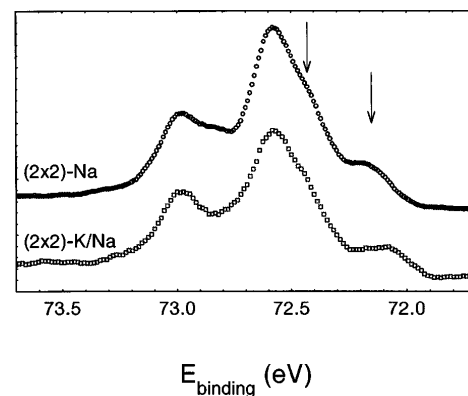


FIG. 3. Al-2*p* core level spectra. The upper and lower curves are for Al(111)- (2×2) -Na and Al(111)- (2×2) -K/Na phases, respectively. The extra spectral features resulting from adsorption of Na and K are marked by arrows.

TABLE I. Na-2*p* energies. The binding energies correspond to the peak positions of the unresolved spin-orbit doublet.

Phase	Na-2 <i>p</i> binding energies (eV)	
$(\sqrt{3} \times \sqrt{3})R30^\circ\text{-Na}$		30.78
$(2 \times 2)\text{-Na}$	30.42	30.93
$(2 \times 2)\text{-Na/K}$	30.36	
$(2 \times 2)\text{-Na/Rb}$	30.31	
$(2 \times 2)\text{-Na/Cs}$	30.35	

as is produced by the reverse adsorption sequence. This conclusion is reinforced by the observation that the Na adsorption leads to a shift in the K-3*p* level from 18.10 to 18.30 eV, consistent with the reduced K/Al coordination of K atoms in the outer layer of the $(2 \times 2)\text{-Na/K}$ structure as compared with that of K atoms in the $\sqrt{3}\text{-K}$ structure. We note also that LEED intensity-energy spectra measured for the $(2 \times 2)\text{-Na/K}$ phases formed by the two adsorption sequences are identical.

Similar results were found for the $(2 \times 2)\text{-Na/Rb}$ and $(2 \times 2)\text{-Na/Cs}$ phases formed by coadsorption of 1/4 ML Na with 1/4 ML Rb or Cs, leading to the conclusion that the structures of these phases are qualitatively the same as that of the $(2 \times 2)\text{-Na/K}$ phase shown in Fig. 1, except that the outer layer consists of Rb and Cs, respectively. These results will be discussed in detail elsewhere, but we list here the measured Na-2*p* binding energies for all of the $(2 \times 2)\text{-Na/X}$ phases in Table I.

LEED intensity-energy spectra were measured at normal incidence and at 100 K after preparation of the $(2 \times 2)\text{-Na/X}$ phases by coadsorption at room temperature. For each system, spectra were measured for 14 symmetry-inequivalent beams in the energy range 50–450 eV. The surface structures were refined by an iterative minimization of the *R* factor for the fit between experimental and calculated spectra as a function of the positions and isotropic vibrational amplitudes of atoms in the first six layers, using procedures described elsewhere [11,16]. Intensity spectra were calculated using 14 phase shifts, derived from the muffin-tin potentials of Moruzzi, Janak, and Williams [24] for Al, Na, K, and Rb, and from a linear muffin-tin orbital potential [25] for Cs, and using 313 beams, reduced by the symmetry of normal incidence to 62 beams.

In the following we limit our discussion to the results of an analysis of the $(2 \times 2)\text{-Na/K}$ phase. The results for the corresponding $(2 \times 2)\text{-Na/Rb}$ and $(2 \times 2)\text{-Na/Cs}$ phases are quite similar and will be discussed in detail elsewhere. It should be emphasized that the existence of a qualitative model of the surface structures, as provided by the core level measurements, was indispensable in carrying out the LEED analysis. In particular, the strong evidence from the core level measurements that Na and X atoms are present in separate layers was critical. The occurrence of *mixed* Na/X layers might well have precluded a definitive LEED result.

The results of the refinement of the model of Fig. 1 are given in Table II. A comparison of experimental LEED intensity-energy spectra with spectra calculated for the tabulated best-fit parameter values is shown in Fig. 4 for 5 of the 14 symmetry-inequivalent beams used in the analysis. The level of agreement between experiment and theory (*R* = 0.064) is not far from the reproducibility of the experimental data (*R* = 0.023 for the comparison of experimental symmetry-equivalent beams) and compares well with the level of agreement (*R* = 0.039) obtained previously for the simpler $(2 \times 2)\text{-Na}$ structure [12], giving a high degree of confidence in the correctness of the model.

In summary, analyses of core level binding energies and LEED intensity-energy spectra provide a consistent description of the $(2 \times 2)\text{-Na/X}$ structures formed by coadsorption of Na and X \equiv K, Rb, Cs on Al(111). The structures are shown to consist of X-Al-Na sandwiches on a reconstructed Al substrate. The layer geometry of the X-Al-Na sandwiches, like that of the $(2 \times 2)\text{-Na}$ structure [12,16], is similar to that of the bcc CsCl structure widely adopted by binary alloys [26]. Thus we regard the structures as *surface ternary alloys*. We believe that the present work is the first documentation for the existence of this class of surface structure. We suggest that the observed invariance of the $(2 \times 2)\text{-Na/X}$ structures to the coadsorption sequence can be attributed to the larger binding energy for Na, as compared to K, Rb, or Cs, in the sixfold coordinated substitutional sites in the reconstructed first layer of the Al substrate [17].

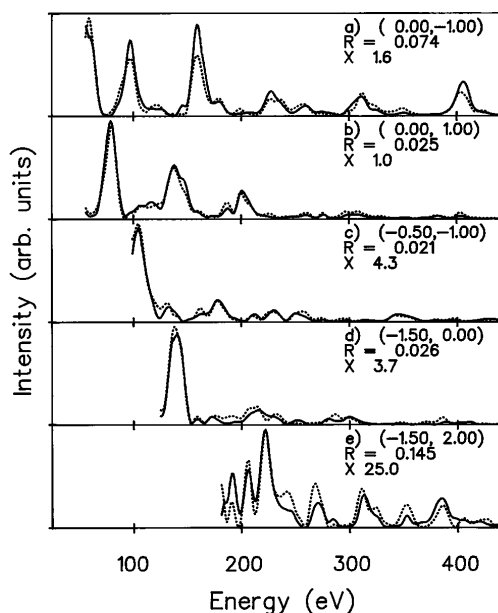


FIG. 4. Experimental LEED intensity-energy spectra (full lines) for 5 of the 14 beams measured at normal incidence compared with spectra (dotted lines) calculated for the model of Fig. 1 with geometry specified in Table II. A *single* scale factor has been used to normalize the experimental and calculated intensities for all 14 beams. Beam *hk* indices, *R* factors, and plot scale factors are given in the figure.

TABLE II. Interlayer spacings, relaxations, and isotropic vibrational amplitudes determined by LEED for the structure of Al(111)-(2 × 2)-Na/K (see Fig. 1). The three Al atoms in the (2 × 2) unit cell of the reconstructed Al layer, which form the site for Al atoms in the sandwich layer, move laterally $\Delta a_{\text{Al, recon}}$ away from the projected positions of Al atoms in the sandwich layer. The Al atoms in the first bulk layer that lie directly beneath Al atoms in the sandwich layer move in the direction of the bulk by $\Delta z_{\text{Al, bulk1}}$ with respect to the remaining atoms of the layer. Thus the first bulk Al layer is rumpled, with a separation $\Delta z_{\text{Al, bulk1}}$ between two bilayers. The layer spacings $d_{\text{Al, recon-Al, bulk1}}$ and $d_{\text{Al, bulk1-Al, bulk2}}$ are given with respect to the midpoint of this rumpled layer.

Interlayer spacings and relaxations (Å)		Vibrational amplitudes (Å)	
$d_{\text{K-Al, sand}}$	1.37 ± 0.03	u_{K}	0.25 ± 0.03
$d_{\text{Al, sand-Na}}$	0.65 ± 0.03	$u_{\text{Al, sand}}$	0.16 ± 0.04
$d_{\text{Na-Al, recon}}$	1.40 ± 0.03	u_{Na}	0.20 ± 0.04
$\Delta a_{\text{Al, recon}}$	0.05 ± 0.05	$u_{\text{Al, recon}}$	0.10 ± 0.03
$d_{\text{Al, recon-Al, bulk1}}$	2.26 ± 0.03		
$\Delta z_{\text{Al, bulk1}}$	0.03 ± 0.03	$u_{\text{Al, bulk1}}$	0.10 ± 0.03
$d_{\text{Al, bulk1-Al, bulk2}}$	2.28 ± 0.03		
$d_{\text{Al, bulk2-Al, bulk}}$	2.35 ± 0.03	$u_{\text{Al, bulk}}$	0.09 ± 0.03

This larger binding energy provides the driving force for Na atoms to burrow under a preadsorbed layer of K, Rb, or Cs.

The authors acknowledge many useful discussions with Jesper Andersen. This work was supported by the Danish Natural Science Research Council.

*Permanent address: Department of Chemistry, University of Copenhagen, Universitetsparken 5, DK-2100 København Ø, Denmark.

- [1] A. Schmalz, S. Aminpirooz, L. Becker, J. Haase, J. Neugebauer, M. Scheffler, D.R. Batchelor, D.L. Adams, and E. Bøgh, *Phys. Rev. Lett.* **67**, 2163 (1991).
- [2] C. Stampfl, M. Scheffler, H. Over, J. Burchhardt, M.M. Nielsen, D.L. Adams, and W. Moritz, *Phys. Rev. Lett.* **69**, 1532 (1992); *Phys. Rev. B* **49**, 4959 (1994).
- [3] J.N. Andersen, M. Qvarford, R. Nyholm, J.F. van Acker, and E. Lundgren, *Phys. Rev. Lett.* **68**, 94 (1992).
- [4] M. Kerkar, D. Fisher, D.P. Woodruff, R.G. Jones, R.D. Diehl, and B. Cowie, *Phys. Rev. Lett.* **68**, 3204 (1992).
- [5] J.N. Andersen, E. Lundgren, R. Nyholm, and M. Qvarford, *Phys. Rev. B* **46**, 12 784 (1992).
- [6] S. Aminpirooz, A. Schmalz, L. Becker, N. Pangher, J. Haase, M.M. Nielsen, D.R. Batchelor, E. Bøgh, and D.L. Adams, *Phys. Rev. B* **46**, 15 594 (1992).
- [7] M. Kerkar, D. Fisher, D.P. Woodruff, R.G. Jones, R.D. Diehl, and B. Cowie, *Surf. Sci.* **278**, 246 (1992).
- [8] J.N. Andersen, E. Lundgren, R. Nyholm, and M. Qvarford, *Surf. Sci.* **289**, 307 (1993).
- [9] A. Schmalz, S. Aminpirooz, J. Haase, D.R. Batchelor, M.M. Nielsen, E. Bøgh, and D.L. Adams, *Surf. Sci.* **301**, L211 (1994).
- [10] M.M. Nielsen, J. Burchhardt, D.L. Adams, E. Lundgren, and J.N. Andersen, *Phys. Rev. Lett.* **72**, 3370 (1994).
- [11] J. Burchhardt, M.M. Nielsen, D.L. Adams, E. Lundgren, and J.N. Andersen, *Phys. Rev. B* **50**, 4718 (1994).
- [12] J. Burchhardt, M.M. Nielsen, D.L. Adams, E. Lundgren, J.N. Andersen, C. Stampfl, M. Scheffler, A. Scmalz, S. Aminpirooz, and J. Haase, *Phys. Rev. Lett.* **74**, 1617 (1995).
- [13] J. Wang, Z.C. Ying, and E.W. Plummer, *Phys. Rev. B* **51**, 5590 (1995).
- [14] W. Berndt, D. Weick, C. Stampfl, A.M. Bradshaw, and M. Scheffler (to be published).
- [15] J.N. Andersen, *Surf. Rev. Lett.* **2**, 345 (1995).
- [16] D.L. Adams, *Appl. Phys. A* **62**, 123 (1996).
- [17] J. Neugebauer and M. Scheffler, *Phys. Rev. B* **46**, 16 067 (1992).
- [18] J. Neugebauer and M. Scheffler, *Phys. Rev. Lett.* **71**, 577 (1993).
- [19] C. Stampfl, J. Neugebauer, and M. Scheffler, *Surf. Sci.* **307**, 8 (1994).
- [20] C. Stampfl and M. Scheffler, *Surf. Sci.* **319**, L23 (1994).
- [21] C. Stampfl and M. Scheffler, *Surf. Rev. Lett.* **1**, 222 (1994).
- [22] C. Stampfl and M. Scheffler, *Surf. Rev. Lett.* **2**, 317 (1995).
- [23] E. Uggerhøj, *Nucl. Instrum. Methods Phys. Res. B* **99**, 261 (1995).
- [24] V.L. Moruzzi, J.F. Janak, and A.R. Williams, *Calculated Electronic Properties of Metals* (Pergamon, New York, 1978).
- [25] N.E. Christensen (private communication).
- [26] P. Villars and L.D. Calvert, *Pearson's Handbook of Crystallographic Data for Intermetallic Phases* (ASM International, Materials Park, Ohio, 1991).